

Current correlators in QCD: OPE versus large distance dynamics.

V.I.Shevchenko and Yu.A.Simonov

State Research Center

*Institute of Theoretical and Experimental Physics, B.Chermushkinskaya 25
117218 Moscow, Russia*

e-mail: shevchen,simonov@itep.ru

Abstract

We analyse the structure of current-current correlators in coordinate space in large N_c limit when the corresponding spectral density takes the form of an infinite sum over hadron poles. The latter are computed in the QCD string model with quarks at the ends, including the lowest states, for all channels. The corresponding correlators demonstrate reasonable qualitative agreement with the lattice data without any additional fits. Different issues concerning the structure of the short distance OPE are discussed.

1 Introduction

Correlators of hadron currents (denoted as CC in what follows)

$$\mathcal{P}^{(c)}(x) = \langle j^{(c)}(x)j^{(c)}(0)^\dagger \rangle \quad (1)$$

are the basic elements in QCD which have been studied in the framework of perturbation theory [1] and also using the Operator Product Expansion (OPE) [2]. More recently CC have been the subject of exciting lattice calculations [3, 4] as a tool to study nonperturbative vacuum configurations. Since then it has been realized that CC can provide information of two sorts: a) one is encoded in the hadron mass poles m_n^2 and quark coupling constants c_n and can be associated with the long distance dynamics (LDD), b) another kind of information can be extracted from the behavior of $\mathcal{P}^{(c)}(x)$ at small x (or at large Q^2 from the Fourier transform $\mathcal{P}^{(c)}(Q)$) with the help of the OPE (see, e.g. [5]) where the coefficients represent vacuum matrix elements of local field operators. Since OPE is assumed to be valid at small distances, one can associate it with what we shall call the short distance dynamics (SDD).

There is another way to stress these two different facets of CC analysis. In the standard Shifman-Vainshtein-Zakharov (SVZ) framework [2] one proceeds in two steps. First, the CC is expanded in local products of fields and, second, the matrix elements of the latter over (nonperturbative) vacuum states are taken. However, in principle one can go the other way: first, to take an average of the CC over the vacuum and, as a second step, to expand the result in power series at small distances. In the former case the answer is written in terms of the SVZ vacuum condensates (like $\langle G_{\mu\nu}^2 \rangle$ or $\langle \bar{\psi}\psi \rangle$), while in the latter case one has to deal with the spectral parameters (like string tension σ , masses etc.). It is often assumed in the literature that the results of the two procedures outlined above must coincide identically. This is an important element of the SVZ sum rules: keeping only a few lowest terms in expansions of *both* kinds, one puts them equal to each other and with the help of some additional mathematical tricks (Borel transformation) the spectral parameters of low lying resonances can be expressed in terms of universal vacuum characteristics like quark and gluon condensates. From the qualitative point of view, the approach forbids the so called λ^2/Q^2 term (see discussion in [6]) since no local gauge-invariant dimension 2 operator exists in QCD. On the other hand, it is easy to get nontrivial term of this kind (for example, $\lambda^2 \sim \sigma$) from the spectral expansion point of view.

The two approaches just described have an important physical difference. The standard OPE framework encodes the knowledge about confinement properties of the theory in very indirect way, via condensates etc. However, nonzero vacuum expectation value of some local gauge-invariant operator by itself does not imply confinement since the latter is essentially nonlocal phenomenon linked with the structure of asymptotic states of the theory.¹ On the other hand, the spectral expansion manifestly takes this aspect into account. One can

¹This is also true on the lattice where confinement criteria such as area law or linearly rising potential are physically meaningful only for times/distances larger than some typical nonperturbative scale.

say that the standard condensate series is surely sensitive to nonperturbative physics of the theory but at the same time is "confinement-blind" at the level of a few lowest terms, since confinement is expected to arise after summation of the whole series.

In our opinion, there are no solid reasons for the mentioned coincidence between SDD and LDD to take place beyond perturbation theory. The key point here is divergence of the series in question. This precludes to construct one-to-one correspondence between terms of the small distance expansions based on LDD and on SDD. In general case each term of the expansion based on LDD is a result of some SDD subseries summation and vice versa (see examples in [7]). Moreover, strictly speaking one needs an additional prescription to assign physical meaning to the (divergent) sum of matrix elements of local operators. We do not address general issues of the OPE structure here, leaving this problem for future publications (see also [8] and references therein in this respect). Instead we shall compare below the explicit expression of CC in LDD at large N_c with the lattice data [3, 4]. These data provide an essential information on CC in the range $0 \leq x \leq 1.5$ fm where both LDD and SDD are present and therefore one may check in principle i) the region of validity of the standard OPE, ii) the transition region from SDD to LDD and the quark-hadron duality (QHD), iii) the validity of specific vacuum models and finally iv) the validity of LDD.

In the latter case one has large N_c limit where there is a solid knowledge of the spectrum properties [9]. Some aspects of OPE at large N_c have been discussed recently in [10]. Let us remind that the masses and residues (properly normalized) of CC , m_n and c_n , are stable at large N_c limit, and recent lattice data (see [11] and references therein) confirm that typically corrections to stable quantities for $N_c = 4, \dots, 8$ are small.² Moreover at large N_c one can in principle compute the hadron spectrum (i.e. the set of m_n, c_n) quasiclassically in analytic form for all n and thus calculate CC explicitly. This was done for the masses (see [12] and references therein) and the residues ([13], see also [14]) and compared in [15] with OPE, SVZ sum rules and experiment. In doing so one encounters and solves several important problems, which we briefly comment on below.

First, the knowledge of m_n, c_n at large N_c allows to find the limit of the CC at large Q (small x) and compare it with the quark-partonic expression, thus checking the quark-hadron duality which was suggested long ago and studied since then in numerous works (see reviews [16] containing extensive lists of references to the original papers).

Secondly, the large N_c LDD provides the small x OPE with coefficients depending only on the string tension σ , and this LDD OPE is to be distinguished from the standard, or SDD OPE. These two types of OPE are in principle distinct, however in the vector channel both agree with the experimental e^+e^- data, as was shown in [15]. Many efforts have been undertaken to match these OPE's (see, e.g. [18, 19, 20]), but here we do not follow this line.

Thirdly, one has a unique chance to compare theoretical values of CC in LDD with experiment and lattice data and discover its region of validity.

²In what follows the flavour-singlet channels where corrections can be large, are not considered.

Since theoretical CC in LDD contain no adjustable parameters at all, and are computed in terms of fixed values of σ and α_s only (and final forms of CC contain only two fixed masses, expressed through σ, α_s) this comparison has a form of a fixed prediction.

The main purpose of this letter is to construct explicit expressions for CC in large N_c LDD in the Euclidean 4d x -space and to compare those with lattice results from [3] and [4]. This is done in sections 2 and 3. The data from [3] we are going to compare with were obtained on $16^3 \times 24$ lattice with the spacing 0.17 Fm and $\beta = 5.7$, while the author of [4] used the lattice of the total size 1.5 Fm and the spacing 0.13 Fm at $\beta = 5.9$. Both simulations were performed in quenched approximation, however the current fermions were taken into account differently. An interested reader is encouraged to consult the original papers [3, 4] for all technical details concerning the simulations.

In section 3 we calculate the LDD OPE as the Taylor x -expansion and compare it to the standard OPE and lattice data, defining in this way regions of validity of the corresponding expansions. There are a few subtle points of difference between OPE in the coordinate space and in the momentum space, stated already in the original papers [2, 21] and discussed also in [22]. We are not going to repeat old arguments here and refer an interested reader to the corresponding literature. The fourth section is devoted to discussion of the results and to a short summary of possible perspectives.

2 The model

The model of zero-width equidistant resonances [23, 24, 25] has been analyzed in different respects in connection with OPE and large N_c QCD, where the main interest has been concentrated on the momentum-space representation [18, 19]. We are following a different path, keeping ourselves in coordinate space.

As it is discussed in the Introduction, in order to get an information about nonperturbative contents of the current correlators in QCD one usually proceeds along one of two ways. The first one starts from the small distances - due to asymptotic freedom it is safe to assume that the leading term at small enough distances is given by the perturbation theory. There must be power corrections however, and at this moment the standard method of SVZ comes into play. The second way goes from the large distances. Because the theory in question is by assumption confining, at large distances current-current correlator is dominated by exchange of the lightest excitation with the particular quantum numbers. When distance is decreasing, the contribution of higher states is turning on and at intermediate distances the whole tower of states plays role. We choose the latter way to go in what follows. The main object of our interest is the current-current correlator in coordinate space given by (1), where the current $j^{(c)}(x) = \bar{\psi}(x)\Gamma_c\psi(x)$ is defined for the given channel c . We consider only flavor nonsinglet charged currents (of the type $\bar{u}\Gamma d$) in this paper. The matrix Γ_c carries Lorentz, flavor and color indices (with the latter structure being always $\delta_{\alpha\beta}$), corresponding

to quantum numbers of the channel c . So we have for vector (ρ - channel), axial (a_1 - channel), pseudoscalar (π - channel) and scalar (a_0 - channel) the following expressions for the (charged) currents

$$j_\mu^{(v)}(x) = \bar{u}\gamma_\mu d; \quad j_\mu^{(a)}(x) = \bar{u}\gamma_\mu\gamma_5 d; \quad j^{(p)}(x) = \bar{u}i\gamma_5 d; \quad j^{(s)}(x) = \bar{u}d \quad (2)$$

We adopt the standard normalization of [1, 2], which is different for neutral currents by a factor $1/\sqrt{2}$ from the one used in [5].

It is convenient to factor out the free part of the correlator (1) and to define the ratio $R^{(c)}(x)$ as

$$R^{(c)}(x) = \frac{\mathcal{P}^{(c)}(x)}{\mathcal{P}_{free}^{(c)}(x)} \quad (3)$$

where by definition for the vector and axial channels the sum over Lorentz indices is always taken:

$$\mathcal{P}^{(v,a)}(x) = g^{\mu\nu} \mathcal{P}_{\mu\nu}^{(v,a)}(x) \quad (4)$$

The free part $\mathcal{P}_{free}^{(c)}(x)$ is given by the following expression in the chiral limit:

$$\mathcal{P}_{free}^{(v,a,p,s)}(x) = \frac{N_c}{\pi^4 x^6} \cdot (2, 2, -1, -1) \quad (5)$$

The important relation $R^{(c)}(x)$ has to obey is given by

$$\lim_{x \rightarrow 0} R^{(c)}(x) = 1 \quad (6)$$

Its physical interpretation depends on what point of view - SDD or LDD - one takes. In the former case the fact that all effects of interaction - perturbative and nonperturbative - switches off at small distances is what is commonly known as asymptotic freedom. The interpretation is more subtle in the latter case - the fact that the whole tower of hadron states gives total contribution coinciding with that of the free quarks (at small distances) is one of manifestations of the quark-hadron duality. From the point of view of the spectral expansion, duality is a highly nontrivial phenomenon since it puts severe bounds on the properties of $\{m_n\}$, $\{c_n\}$ at $n \rightarrow \infty$. In principle, one should be able *to derive*, rather than *postulate* quark-hadron duality for each given channel starting, for example, from (relativistic) Hamiltonian and computing its spectrum in this channel. This problem is beyond the scope of our paper and will be considered elsewhere. Instead we will always assume quark-hadron duality in what follows and fix the coefficients $\{c_n\}$ to yield duality. In other words, the condition (6) holds by definition in our approach.

Another problem is the perturbative corrections. As a matter of principle, the LDD procedure remains the same, but one is to include in the spectral sum hybrid states. The fact that diagrams of perturbative corrections in confining vacuum are connected to the hybrid excitations was discovered in [26] and discussed in [15], see also [27, 28]. At small distances n -gluon hybrid excitation would correspond to the perturbative correction $O(\alpha_s^n)$

from the SDD point of view. It is an interesting open problem to establish this relation in explicit way and we leave it beyond the scope of this paper. The lattice data we are mainly focused on provide no clear indication of such corrections as well as of any effects caused by perturbative running.³ The same reasoning is applicable to anomalous dimensions for nonconserved currents we take no care of in what follows.

We find it instructive to explain our attitude, which in some respects is different from that of the cited papers [18, 19, 20]. Our basic assumption is that QCD exhibits confinement in the form of minimal area law in large N_c limit. Since we always have in mind large N_c , the picture of zero-width states is justified and the confinement property guarantees the spectrum to be discrete. On the other hand, thanks to the area law one is able to solve the corresponding Hamiltonian problem for two masses (quarks) connected by the minimal string [17] and to get equidistant spectrum (at least quasiclassically), as it was done in [12]. Therefore for each channel we are dealing with the corresponding set of poles $\{m_n\}$ and residues $\{c_n\}$ which in a sense completely characterizes the theory. We get for the imaginary part of polarization operator

$$\frac{1}{\pi} \text{Im} \Pi(s) = \sum_{n=0}^{\infty} c_n \cdot \delta(s - m_n^2) \quad (7)$$

This is the basic expression we are to work with below.

The mass spectrum is obtained quasiclassically to have the following form [15, 17, 29]

$$m_n^2 = m_0^2 + m^2 n \quad (8)$$

where the quantity m^2 is defined universally for all channels to be $m^2 = 4\pi\sigma$ as it was found by the quasiclassical analysis (see also [31] and references therein). Here σ is physical string tension. The residues for the ground state and the excited states are treated differently. As for the latter, they are fixed by the requirement of quark-hadron duality. The lowest state residue is chosen in different physically motivated ways for different channels (see below). Our approach is phenomenological in this respect, since we have not computed all c_n starting from some consistent theoretical scheme (it will be done elsewhere). It is worth stressing however, that we do not perform any kind of fitting procedure. In some sense, we have no fitting parameters at all in our formulas since all quantities like m_0 , σ take their physical values. We do not try to fit the lattice data, instead, we use them for comparison with the results of quasiclassical spectrum of large N_c QCD.

2.1 Vector channel

For conserved vector current one can write the following expression in momentum space

$$\mathcal{P}_{\mu\nu}^{(v)}(q) = i \int d^4x \mathcal{P}_{\mu\nu}^{(v)}(x) \exp(iqx) = (q_\mu q_\nu - q^2 g_{\mu\nu}) \Pi^{(v)}(q^2) \quad (9)$$

³For example, due to asymptotic freedom $R^{(c)}(x)$ should approach unity logarithmically slow when $x \rightarrow 0$, which is not seen on the lattice, as figures 1.1 - 4.1 clearly demonstrate.

and the determination of $\Pi^{(v)}(q^2)$ for $-q^2 = Q^2 > 0$ is of interest.

It was shown in [13, 15, 17] that for a system made of relativistic quarks connected by the straight-line string with tension σ one has

$$m_n^2 = 2\pi\sigma(2n_r + L) + m_0^2 \quad ; \quad c_n = \frac{N_c}{12\pi^2} \cdot 4\pi\sigma \quad (10)$$

which leads to

$$\Pi^{(v)}(-Q^2) = \frac{\lambda_\rho^2}{Q^2 + m_0^2} + \frac{N_c}{12\pi^2} \sum_{n=1}^{\infty} \frac{a_n}{Q^2 + m_n^2} \quad (11)$$

where

$$m_n^2 = m^2 n + m_0^2 \quad ; \quad a_n = m^2 = 4\pi\sigma \quad (12)$$

Despite we work in the large N_c framework, we have kept the factor N_c in front of the second term in (11) in order to make contact with the asymptotic expression (13). The residue of the first (ρ -meson) pole should in principle be calculated in the same dynamical framework, which is used for the spectrum calculation.⁴ The condition (10) provides the quark-hadron duality in this channel:

$$\Pi^{(v)}(-Q^2) \xrightarrow{Q^2 \rightarrow \infty} -\frac{N_c}{12\pi^2} \log\left(\frac{Q^2}{\mu^2}\right) \quad (13)$$

Numerically we use values $m_0^2 = M_\rho^2 = 0.6 \text{ GeV}^2$, $\lambda_\rho^2 = 0.047 \text{ GeV}^2$ and $m^2 = 4\pi\sigma = 2.1 \text{ GeV}^2$, corresponding to $\sigma = 0.17 \text{ GeV}^2$. The value of λ_ρ^2 is consistent with the one used in [5, 20] and also the one computed in [30]. Notice that in the latter case we are not to take into account the large $O(\alpha_s)$ correction which is not seen in lattice simulations. It is interesting that the value of the lowest state residue λ_ρ^2 is different from the asymptotic value c_n by less than 15% in our case.

Since we want to compare our model with the lattice results, the Wick rotation has to be performed. See Appendix B where all relevant formulas are collected. The resulting expression in coordinate space, corresponding to (11) is given by:

$$R^{(v)}(z) = \xi z^5 K_1(z) + \frac{bz^6}{27} \bar{p}_b(z) \quad (14)$$

where dimensionless distance $z = x_E m_0$ and mass ratio $b = m^2/m_0^2$ have been introduced and

$$\xi = \frac{\pi^2}{8} \left(\frac{\lambda_\rho^2}{m_0^2} - \frac{b}{4\pi^2} \right) \quad (15)$$

The universal function $\bar{p}_b(z)$ is given by

$$\bar{p}_b(z) = \int_0^\infty \frac{du}{u^2} \exp\left(-\frac{z^2}{4u} - u\right) \frac{1 + \exp(-bu)(b-1)}{(1 - \exp(-bu))^2} \quad (16)$$

⁴This is also true for higher resonances, however, we choose another way and fix those residues by quark-hadron duality for those channels where c_n have not yet been calculated dynamically. Notice that in some channels like the vector one, dynamically calculated c_n indeed provide quark-hadron duality (see [31]).

As it has already been mentioned, we have three parameters in the expression (14): m_0 , which fixes the overall scale of distance, λ_ρ^2 and b characterizing the spectrum, and all of them are fixed by their physical values. The resulting plot is shown on Figs. 1.1 and 1.2, to be compared with the lattice data of [3] and [4], respectively. One sees reasonable qualitative agreement with the lattice data. In fact, the results from [3] and from [4] were obtained for different lattice parameters (see the cited papers for details) and strictly speaking they do not agree with each other at large distances. However the qualitative agreement takes the place, and both sets of data reasonably correspond to our simple expression (14).

Of separate interest is the short distance limit of our results. It is straightforward to expand (14) near $z = 0$, the answer is (see Appendix B)

$$R^{(v)}(z) = \left[\xi z^4 + \frac{\xi}{4} z^6 \log z^2 + \dots \right] + \left[1 + \frac{1}{3 \cdot 2^7} (6b - 6 - b^2) z^4 + \frac{3b - 2 - b^2}{3 \cdot 2^8} z^6 \log z^2 + \dots \right] \quad (17)$$

The first and the second brackets in the r.h.s. of (17) correspond to the first and the second terms in the r.h.s. of (14), respectively. The dots stay for higher order terms.

Notice an absence of a term proportional to z^2 in (17). It is easy to see by dimensional reasons that such term would correspond to λ^2/Q^2 contribution in the polarization operator (11). Indeed, high momentum asymptotics of (11) reads:

$$\begin{aligned} \Pi^{(v)}(-Q^2) &= \frac{N_c}{12\pi^2} \left[-\log \left(\frac{Q^2}{m^2} \right) + \left(4\pi^2 \lambda_\rho^2 - \frac{1}{2} m^2 - m_0^2 \right) \cdot \frac{1}{Q^2} + \right. \\ &\quad \left. + \left(\frac{1}{2} m_0^4 + \frac{1}{2} m^2 m_0^2 + \frac{1}{12} m^4 - 4\pi^2 \lambda_\rho^2 m_0^2 \right) \cdot \frac{1}{Q^4} + O(Q^{-6}) \right] \end{aligned} \quad (18)$$

so it generally contains $1/Q^2$ term (and in this sense violate the standard OPE where such term is absent). In coordinate space, however, this term being multiplied by Q^2 produces delta-function like contribution which we systematically disregard in this paper. In this sense it is impossible to detect $1/Q^2$ term by simulation of the correlator in coordinate space (it was noticed in [32]). However, one may take a different attitude and put the requirement $\lambda^2 = 0$ right on the momentum space expression (18). This would lead to a certain relation between different parameters of the model, in our case it is $64\xi = 2 - b$. If one takes all residues equal (i.e. with $\xi = 0$), it changes to the standard value $b = 2$. It is interesting to notice that for the parameters we have actually chosen λ^2 defined by

$$-\frac{\alpha_s}{4\pi^3} \lambda^2 = \lambda_\rho^2 - \frac{1}{4\pi^2} \left(\frac{1}{2} m^2 + m_0^2 \right) \quad (19)$$

is equal to $\frac{\alpha_s}{\pi} \lambda^2 = -0.2 \text{ GeV}^2$ which is still "tachyonic", to be compared with $\frac{\alpha_s}{\pi} \lambda^2 = -(0.07 - 0.09) \text{ GeV}^2$ from [6].

For the sake of completeness let us also cite the standard OPE answer for the discussed correlator (for the physical value $N_c = 3$) [5, 32]:

$$R^{(v)}(\tau) = 1 + \frac{\alpha_s(\tau)}{\pi} - \frac{\langle (gG_{\mu\nu}^a)^2 \rangle}{3 \cdot 2^7} \tau^4 - \frac{7\pi^3}{81} \alpha_s \langle \bar{q}q \rangle^2 \tau^6 \log \tau^2 \mu_v^2 + \dots \quad (20)$$

where τ is Euclidean time coinciding with x_E in our case. We use the standard values

$$\langle (gG_{\mu\nu}^a)^2 \rangle = 0.5 \text{GeV}^4 \quad ; \quad |\langle \bar{q}q \rangle| = (250 \text{MeV})^3 \quad (21)$$

It is worth noticing⁵ that the expression (20) contains a contact term $\langle j^\mu j_\nu \rangle$ which is not directly seen in the momentum space. This term's contribution is proportional to the sixth power of τ in (20), on the other hand, there is no α_s in front of it [22]. Numerically according to [22]

$$\langle \bar{u} \gamma_\mu d \bar{d} \gamma^\mu u \rangle / \langle \bar{q}q \rangle^2 = -\frac{1}{3} (0.90 \pm 0.15)$$

We take this circumstance into account by means of numerical redefining μ_v^2 in (20) accordingly, while still keeping the expression in the form (20). In fact, our main concern is to compare (14) with the lattice, while we need (20) mostly for illustrative purposes.

On Fig. 1.3 we compare the exact expression (14) with its own short distance expansion (17) and also with the conventional OPE result (20) where the three power terms have been kept in both cases. The Figure 1.3 shows striking difference from the Figs. 1.1, 1.2. Sizeable deviations of the standard OPE from (14) start as early as at $x \approx 0.4$ Fm. We have also plotted the first resonance contribution the answer should converge to at large distances. The sum over resonances smoothly interpolates between small and large distance regions.

2.2 Axial channel

We are now to consider the axial channel. Some care is needed here since one has to extract the pion contribution. There are two Lorentz structures in this channel

$$\mathcal{P}_{\mu\nu}^{(a)}(q) = i \int d^4x \mathcal{P}_{\mu\nu}^{(a)}(x) \exp(iqx) = (q_\mu q_\nu - g_{\mu\nu} q^2) \Pi_1(q^2) + q_\mu q_\nu \Pi_2(q^2) \quad (22)$$

Contracting both sides with the tensor $q_\mu q_\nu$ one gets (see Appendix A):

$$q_\mu q_\nu \mathcal{P}_{\mu\nu}^{(a)}(q) = q^4 \Pi_2(q^2) = 2(m_u + m_d) \langle \bar{u}u + \bar{d}d \rangle + (m_u + m_d)^2 \bar{\mathcal{P}}^{(p)}(q^2) \quad (23)$$

We have put the bar over $\mathcal{P}^{(p)}(q^2)$ in order to stress that we keep only the pion pole contribution in the pseudoscalar correlator in (23) (compare with the whole tower taken into account in (34)). This is consistent with the use of Gell-Mann – Oakes – Renner relation

⁵The authors are indebted to Prof. K.G.Chetyrkin for discussion of this point.

in the standard form and such assumption has approximately the same level of accuracy as this relation itself. So we have

$$\bar{\mathcal{P}}^{(p)}(-Q^2) = \frac{\lambda_\pi^2}{Q^2 + m_\pi^2} \quad (24)$$

where as usual $Q^2 = -q^2$. The pion residue is fixed by PCAC (see Appendix A) as

$$\lambda_\pi^2 = \frac{2f_\pi^2 m_\pi^4}{(m_u + m_d)^2} \quad (25)$$

where we take $f_\pi = 93$ MeV, $m_\pi = 140$ MeV, $m_u + m_d = 11$ MeV, so that $\lambda_\pi^2 = 0.05$ GeV⁴.

In principle, one can address in the same framework the question about corrections to (58) (and correspondingly to (59), (60)) due to higher (nonchiral) or multipion states. This analysis is beyond the scope of the present paper. Notice the overall plus sign in (24) fixed by the negative sign of the quark condensate, see Appendix A. One gets the following expression for $\Pi_2(q^2)$:

$$q^2 \Pi_2(q^2) = \frac{2f_\pi^2 m_\pi^2}{m_\pi^2 - q^2} \quad (26)$$

while for $\Pi_1(q^2)$ we have an expression analogous to (11):

$$\Pi_1(-Q^2) = \frac{N_c}{12\pi^2} \sum_{n=0}^{\infty} \frac{a_n}{Q^2 + m_n^2} \quad (27)$$

where we take $m_0 = M_{a_1} = 1.26$ GeV while the residues coincide with those for the vector channel given by (12). We do not separate the lowest state (a_1 resonance) as we did for the vector channel since in this correlator the role of such state is played by pion. Moreover, as it has already been noticed the asymptotic value for residues is natural to expect to be rather close to the one for the lowest state.

Contraction of Lorentz indices in (22) leads to

$$\mathcal{P}^{(a)}(q^2) = g_{\mu\nu} \mathcal{P}_{\mu\nu}^{(a)}(q) = -3q^2 \Pi_1(q^2) + q^2 \Pi_2(q^2) \quad (28)$$

We have therefore

$$\mathcal{P}^{(a)}(-Q^2) = \frac{2f_\pi^2 m_\pi^2}{m_\pi^2 + Q^2} + 3Q^2 \frac{N_c}{12\pi^2} \sum_{n=0}^{\infty} \frac{a_n}{Q^2 + m_n^2} \quad (29)$$

Fourier transformation to the coordinate space is straightforward, the answer is given by the following expression:

$$R^{(a)}(z) = -\frac{\pi^2}{12} f^2 \gamma^3 z^5 K_1(\gamma z) + \frac{bz^6}{27} \bar{p}_b(z) \quad (30)$$

The following notations have been introduced: $\gamma = m_\pi/m_0$, $f = f_\pi/m_0$. Notice the different sign of pion contribution and that of the tower. The correlator becomes negative at large

distances. On Figs. 2.1 and 2.2 expression (30) is compared with the lattice data from [3] and from [4]. The short distance expansion of (30) is given by

$$R^{(a)}(z) = -\frac{\pi^2}{12} f^2 \gamma^3 \left[\frac{1}{\gamma} z^4 + \frac{\gamma}{4} z^6 \log(\gamma z)^2 + \dots \right] + \left[1 + \frac{1}{3 \cdot 2^7} (6b - 6 - b^2) z^4 + \frac{3b - 2 - b^2}{3 \cdot 2^8} z^6 \log z^2 + \dots \right] \quad (31)$$

while the standard OPE series can be written as

$$R^{(a)}(\tau) = 1 + \frac{\alpha_s(\tau)}{\pi} - \frac{\langle (gG_{\mu\nu}^a)^2 \rangle}{3 \cdot 2^7} \tau^4 + \frac{11\pi^3}{81} \alpha_s \langle \bar{q}q \rangle^2 \tau^6 \log \tau^2 \mu_a^2 + \dots \quad (32)$$

where we again denote x_E as τ and the discussion we had after (21) is also valid here. The comparison of (30), (31) and (32) is presented on Fig. 2.3. One can see that the standard OPE (as well as the short distance expansion (31)) deviates significantly from the lattice data at distances larger than 0.4 Fm, while the full spectral density (30) reproduces the latter smoothly.

2.3 Pseudoscalar channel

This channel contains the light pion which makes it different from the others. The corresponding Hamiltonian analysis should take the chiral nature of pion into account. The resulting spectrum contains the lightest excitation (pion) which is massless in the chiral limit plus a tower of massive states with the masses experiencing chiral shifts, which decrease with n (see [33]). Therefore we proceed as before, separating the lowest state (pion) and fixing the residues of all other poles by the duality requirement. The correlator reads as

$$\mathcal{P}^{(p)}(q) = i \int d^4x \langle 0 | T j^{(p)}(x) j^{(p)}(y)^\dagger | 0 \rangle \exp(iq(x - y)) \quad (33)$$

with $j^{(p)}(x) = \bar{u}(x) i \gamma_5 d(x)$. We take the polarization operator in the following form:

$$\mathcal{P}^{(p)}(-Q^2) = \frac{\lambda_\pi^2}{Q^2 + m_\pi^2} + \sum_{n=1}^{\infty} \frac{a_n^{(p)}}{Q^2 + m_n^2} \quad (34)$$

We neglect the chiral shifts for higher states in what follows and take the spectrum of the tower in the form:

$$m_n^2 = m_1^2 + m^2(n - 1) ; \quad n = 1, 2, \dots \quad (35)$$

where $m_1 = 1.3$ GeV as for $\pi(1300)$ state. The residues $a_n^{(p)}$ should depend on n in such a way that the leading term is linear:

$$a_n^{(p)} = a^{(p)} n + \bar{a}^{(p)} + \mathcal{O}(n^{-1}) \quad (36)$$

This form is dictated by the quark-hadron duality, postulated throughout the paper. However, duality requirement allows to fix only the leading term, $a^{(p)}$, but not the subleading one $\bar{a}^{(p)}$ which plays a role of a free parameter in our analysis. For the coefficient $a^{(p)}$ we obtain

$$a^{(p)} = \frac{N_c}{8\pi^2} m^4 \quad (37)$$

which provides

$$\mathcal{P}^{(p)}(-Q^2) \stackrel{Q^2 \rightarrow \infty}{\rightarrow} \frac{N_c}{8\pi^2} Q^2 \log\left(\frac{Q^2}{\mu^2}\right) \quad (38)$$

The full expression for the correlator's ratio in coordinate space has the form:

$$R^{(p)}(z) = \frac{\pi^2}{12} L^2 \gamma z^5 K_1(\gamma z) + \frac{b^2(a+1) - b}{2^5} z^4 \hat{p}_b(z) + \frac{bz^6}{2^7} \bar{p}_b(z) \quad (39)$$

where we use the following notation:

$$\gamma = \frac{m_\pi}{m_1} ; \quad L^2 = \frac{\lambda_\pi^2}{m_1^4} ; \quad a = \frac{8\pi^2 \bar{a}_p}{3m^4} ; \quad b = \frac{m^2}{m_1^2} ; \quad z = m_1 x_E \quad (40)$$

Notice the relative positive sign of the first and the third terms in the rhs of (39). The parameters γ , L and b are fixed by their physical values while the parameter a is free in our approach, on physical grounds it is reasonable to expect it to be of the order of unity. On Figure 3.1 and 3.2 we plot the function $R^{(p)}(z)$ together with the lattice data for the choice $a = 0$. The Figure 3.4 shows the curves (39) for the choices $a = -1, 0, 2$. Varying a slightly affects intermediate distance behavior of the correlator but does not touch short and long distance asymptotics.

As above, we consider the short distance expansions. For (39) it reads

$$\begin{aligned} R^{(p)}(z) &= \frac{\pi^2}{12} L^2 \gamma \left[\frac{1}{\gamma} z^4 + \frac{\gamma}{4} z^6 \log(\gamma z)^2 + \dots \right] + \left[\frac{b(a+1) - 1}{2^3} z^2 + \dots \right] + \\ &+ \left[1 + \frac{1}{3 \cdot 2^7} (6b - 6 - b^2) z^4 + \frac{3b - 2 - b^2}{3 \cdot 2^8} z^6 \log z^2 + \dots \right] \end{aligned} \quad (41)$$

where dots stay for higher powers of z^2 . In contrast to (17), (31) all non-negative powers of z^2 are present in (41). The conventional OPE answer in this channel has the form (see, e.g. [32]):

$$R^{(p)}(\tau) = 1 + \frac{\langle (gG_{\mu\nu}^a)^2 \rangle}{3 \cdot 2^7} \tau^4 - \frac{7\pi^3}{81} \alpha_s \langle \bar{q}q \rangle^2 \tau^6 \log \tau^2 \mu_p^2 + \dots \quad (42)$$

If one includes the quadratic power correction in the OPE expansion (42), the corresponding relation is to be

$$\frac{\alpha_s \lambda^2}{\pi} = -\frac{b(a+1) - 1}{4} \quad (43)$$

Since a is a free parameter in our approach we can make no reasonable estimate of λ^2 from (43). The other way around, fixing the l.h.s. of (43) by (19) corresponds to the value $a = 0.4$.

The Figure 3.3 shows the exact answer (39) together with the short distance asymptotics (41) and (42). Analogously to the other channels, short-distance expansions break down at $x \approx 0.4$ Fm.

2.4 Scalar channel

This channel is presumably the most complex one since it requires some understanding of the a_0 meson nature,⁶ in particular, the complicated dynamical problem of the role played by the four quark state admixture in these states. However, we do not address this set of questions here since the lattice data of [3] we are going to compare with are obtained in quenched approximation. We also take the set of data corresponding to the largest value of current quark mass used in simulations [4]. We also have in mind large N_c limit, where four quark admixture vanishes. We write therefore

$$\mathcal{P}^{(s)}(-Q^2) = \sum_{n=0}^{\infty} \frac{a_n^{(s)}}{Q^2 + m_n^2} \quad (44)$$

with the corresponding quark-hadron duality condition

$$\mathcal{P}^{(s)}(-Q^2) \xrightarrow{Q^2 \rightarrow \infty} \frac{N_c}{8\pi^2} Q^2 \log \left(\frac{Q^2}{\mu^2} \right) \quad (45)$$

The expression for residues coincides with (36):

$$a_n^{(s)} = a^{(s)} n + \bar{a}^{(s)} + \mathcal{O} \left(\frac{1}{n} \right) \quad (46)$$

and

$$a^{(s)} = \frac{N_c}{8\pi^2} m^4 \quad (47)$$

The result for the ratio $R^{(s)}(z)$ is

$$R^{(s)}(z) = \frac{b(ab-1)}{2^5} z^4 \hat{p}_b(z) + \frac{bz^6}{2^7} \bar{p}_b(z) \quad (48)$$

The notation is standard:

$$a = \frac{8\pi^2 \bar{a}_s}{3m^4} ; \quad b = \frac{m^2}{m_0^2} ; \quad z = m_0 x_E$$

Notice the difference between (48) and (39). In the latter case the π - meson pole stay away from the tower, but the numbering of states still respects the fact that the pion is the lowest, $n = 0$ state. This is in line with [3]. In the scalar channel the tower itself starts from the

⁶Let us remind that we work with $I = 1$ case only, so we have no mixing with the pure glue states and do not consider f_0 meson.

lowest state. This causes $b^2(a+1) - b$ factor in (39) instead of $b(ab-1)$ in (48). Also the parameter b is defined differently. One may check that if mass and residue of the lowest state are chosen in such a way that this state also belongs to the equidistant tower, the expression (48) identically coincides with (39), as it should be.

The standard OPE answer is given by [2]

$$R^{(s)}(\tau) = 1 + \frac{\langle (gG_{\mu\nu}^a)^2 \rangle}{3 \cdot 2^7} \tau^4 + \frac{15\pi^3}{81} \alpha_s \langle \bar{q}q \rangle^2 \tau^6 \log \tau^2 \mu_s^2 + \dots \quad (49)$$

while the short distance expansion of (48) takes the form

$$R^{(s)}(z) = \left[\frac{ba-1}{2^3} z^2 + \dots \right] + \left[1 + \frac{1}{3 \cdot 2^7} (6b - 6 - b^2) z^4 + \frac{3b-2-b^2}{3 \cdot 2^8} z^6 \log z^2 + \dots \right] \quad (50)$$

The Figure 4.1 shows the curve defined by (48) for different values of a against the data from [3]. Unfortunately, the data in this channel are not reliable enough, which can be clearly seen on the Figure 4.2, where the lattice correlator from [4] becomes negative at $x \approx 0.5$ Fm due to lattice artefacts, in contradiction with positivity of the spectral density.⁷ The short distance expansions explode even earlier (see Figure 4.3).

3 Discussion of the results and conclusion

We find the results of comparison of the lattice data and the model to be quite remarkable. It is worth stressing that we have worked with the model of two relativistic quarks connected by the string with the tension σ , which is the only dimensionful parameter of the model. Using this picture, first, the lowest resonance masses were computed in all channels [12] and found to be in reasonable agreement with their experimental values. Second, the quasi-classical asymptotic for the mass spectrum was calculated [17] which has the same pattern for all channels. The latter must provide exact quark-hadron duality, which was explicitly shown in the vector case in [15, 30]. We have plugged these two ingredients into the corresponding spectral density and compared the results with the available lattice simulations [3, 4]. Another comparison is made for the standard SVZ short distance OPE expansion and the corresponding expansion provided by our spectral density. It is shown that they strongly deviate from the full curve (and from the lattice data) for the distances larger than 0.35 – 0.45 Fm, as one could expect.

The main lesson is that one needs quite a few inputs (correct lowest resonance mass, correct lowest resonance residue and correct asymptotic behavior dictated by quark-hadron

⁷The authors are grateful to Prof. De Grand for discussion of the problems in this channel.

duality) to reproduce lattice data in a reasonable way. We have taken these inputs from the large N_c model of QCD string with quarks at the ends [17]. The absence of precise quantitative agreement between our results and the lattice should not disappoint since many effects have been ignored ($1/N_c$ effects, perturbative exchanges etc), notice also that the two sets of lattice data we have used do not agree with each other on quantitative level. On the other hand, qualitative agreement is rather good and certainly better than that of the standard short distance OPE in coordinate space. Notice that we have not performed any fitting of the lattice data, the latter was compared with the curves (14),(30),(39),(48) computed independently. If we had fitted the data with these expressions, the agreement would have been much better.

The next logical step is to compare the predictions of large N_c QCD string model with the data taken from real experiments, i.e. the data on τ - decay rates obtained by ALEPH and OPAL collaborations. The accuracy of the data is much higher than what is possible to reach on the lattice, and this fact provides a challenging task for theory. The τ - decay results have been already addressed in the framework of conventional OPE [34] and in the instanton model [35]. The issues of large N_c limit interpretation of the data have also been discussed [36]. We are going to analyse these data in our framework in a separate publication.

Acknowledgments

The authors are grateful to J.W. Negele and T.A. DeGrand for providing their numerical data and valuable explanations. The authors wish to thank A.V.Nefediev, V.I.Zakharov, K.G.Chetyrkin and A.A.Pivovarov for useful discussions. Support from the Federal programme of Russian Ministry of industry, science and technology 40.052.1.1.1112 and from the grant for scientific schools NS-1774.2003.2 is acknowledged. V.Sh. is thankful to the non-profit "Dynasty" foundation and ICFPM for financial support.

Appendix A

This Appendix contains a textbook material (see, e.g. [1]), however we find it useful for the sake of completeness to rederive here the equation (23) in our conventions. The following expressions for charged axial and pseudoscalar currents have been introduced:

$$j_\mu^{(a)}(x) = \bar{u}(x)\gamma_\mu\gamma_5d(x) \quad ; \quad j^{(p)}(x) = \bar{u}(x)i\gamma_5d(x) \quad (51)$$

Using Dirac equation

$$(i\gamma_\mu(\partial_\mu - igA_\mu(x)) - m)\psi(x) = 0 \quad (52)$$

one gets the well known expression for PCAC:

$$\partial_\mu j_\mu^{(a)}(x) = (m_u + m_d)j^{(p)}(x) \quad (53)$$

Next, one defines the following matrix elements of the currents between vacuum and one pion state

$$\langle 0|j_\mu^{(a)}(x)|\pi(p)\rangle = i\sqrt{2} f_\pi p_\mu \exp(-ipx) \ ; \ \langle 0|j^{(p)}(x)|\pi(p)\rangle = \lambda_\pi \exp(-ipx) \quad (54)$$

Our normalization coincides with [1] but $\sqrt{2}$ different from [5]. Correspondingly, we have $f_\pi = 93$ MeV instead of 131 MeV value for f_π used in [5].

Combining (53) and (54) one gets

$$\lambda_\pi = \frac{\sqrt{2} f_\pi m_\pi^2}{m_u + m_d} \quad (55)$$

Consider now the current-current correlator in momentum space

$$\mathcal{P}_{\mu\nu}^{(a)}(q) = i \int d^4x \langle 0|T j_\mu^{(a)}(x) j_\nu^{(a)}(y)^\dagger|0\rangle \exp(iq(x-y)) \quad (56)$$

Making use of free equal-time anticommutation relations for the quark fields, it is straightforward to obtain:

$$q_\mu q_\nu \mathcal{P}_{\mu\nu}^{(a)}(q) = (m_u + m_d)^2 \mathcal{P}^{(p)}(q^2) + 2(m_u + m_d) \langle \bar{u}u + \bar{d}d \rangle \quad (57)$$

where $\mathcal{P}^{(p)}(q)$ is given by (33). Assuming that in the chiral limit one pion state contribution dominates in the pseudoscalar correlator at $q^2 \rightarrow 0$:

$$\mathcal{P}^{(p)}(q^2) \xrightarrow{q^2 \rightarrow 0} \frac{\lambda_\pi^2}{m_\pi^2} \quad (58)$$

one gets

$$2m_\pi^2 \langle \bar{u}u + \bar{d}d \rangle + (m_u + m_d) \lambda_\pi^2 = 0 \quad (59)$$

which together with (55) is nothing but the Gell-Mann – Oakes – Renner relation

$$(m_u + m_d) \langle \bar{u}u + \bar{d}d \rangle = -f_\pi^2 m_\pi^2 \quad (60)$$

up to the terms of higher order in m_π^2 . Taking into account the definition (22) we come to the expression (23) used in the main text.

Appendix B

We collect here the basic formulas used in the main text. The standard metric conventions, correlator definitions, Fourier transforms are adopted. The free propagator is given by

$$\langle \psi(x) \bar{\psi}(0) \rangle = i \int \frac{d^4q}{(2\pi)^4} \frac{\hat{q} + m}{q^2 - m^2} \exp(-iqx) = \left(i\gamma_\mu \frac{\partial}{\partial x_\mu} + m \right) \frac{m^2}{4\pi^2 z} K_1(mz) \quad (61)$$

for space-like x , where $z = m\sqrt{-x^2}$. Four vectors in Minkowskii and Euclidean spaces are defined as follows:

$$q = (q_0, \mathbf{q}) ; \quad q^2 \equiv q_M^2 = q_0^2 - \mathbf{q}^2 ; \quad Q^2 \equiv q_E^2 = -q_M^2 \quad (62)$$

and we often omit the subscripts E, M if it is not misleading. Notice that the Wick rotation changes the free propagator sign :

$$\mathcal{P}_{free}(x) \sim \frac{1}{(x^2)^3} \rightarrow -\frac{1}{(x_E^2)^3} \quad (63)$$

The Fourier transform for the free propagator is given by (see, e.g. [21]):

$$\int d^4x \frac{1}{(x^2)^3} \exp(iqx) \leftrightarrow i\frac{\pi^2}{8}(-q^2) \log(-q^2) \quad (64)$$

Let us calculate the function $\bar{P}(x)$ we have made use of in the main text. It is defined as follows:

$$\bar{P}(x) = 3i \int \frac{d^4q}{(2\pi)^4} q^2 \sum_{n=0}^{\infty} \frac{1}{-q^2 + m_n^2} \exp(-iqx) \quad (65)$$

where $m_n^2 = m_0^2 + m^2 n$. The sum over n is divergent and the divergent (q^2 - independent) constant term is usually eliminated by renormalization $\Pi(q^2) \rightarrow \Pi(q^2) - \Pi(0)$ in momentum space. We proceed in a different way here, simply interchanging the summation over n and integration over q for $x \neq 0$, having in mind condition (6) then $x \rightarrow 0$. We thus systematically disregard all terms proportional to $\delta(x)$ or derivatives of the delta function. In this way one obtains

$$\bar{P}(x) = -3 \left(-\frac{\partial^2}{\partial x^2} \right) \sum_{n=0}^{\infty} \frac{m_n}{4\pi^2 \sqrt{-x^2}} K_1 \left(m_n \sqrt{-x^2} \right) \quad (66)$$

We switch to the Euclidean notations in the summand (66), with $x_E = \sqrt{-x^2} > 0$. Using integral representation for the McDonald function

$$K_1(w) = \frac{w}{4} \int_0^{\infty} \frac{dt}{t^2} \exp \left(-t - \frac{w^2}{4t} \right) \quad (67)$$

and performing the summation over n

$$\sum_{n=0}^{\infty} \exp \left(-\frac{x_E^2 m_n^2}{4t} \right) = \frac{\exp \left(-\frac{x_E^2 m_0^2}{4t} \right)}{1 - \exp \left(-\frac{x_E^2 m^2}{4t} \right)} \quad (68)$$

we obtain

$$\bar{P}(x) = \frac{3}{16\pi^2} \left(\frac{\partial^2}{\partial x^2} \right) \int_0^{\infty} \frac{dt}{t^2} \exp(-t) f_0 \left(\frac{x_E^2}{t} \right) \quad (69)$$

where

$$f_0\left(\frac{x_E^2}{t}\right) = \sum_{n=0}^{\infty} m_n^2 \exp\left(-\frac{x_E^2 m_n^2}{4t}\right) = \frac{\exp\left(-\frac{x_E^2 m_0^2}{4t}\right)}{\left(1 - \exp\left(-\frac{x_E^2 m^2}{4t}\right)\right)^2} \cdot \left(m_0^2 + (m^2 - m_0^2) \exp\left(-\frac{x_E^2 m^2}{4t}\right)\right) \quad (70)$$

To represent the results in more convenient form we use the notation $z = x_E m_0$ for dimensionless distance and $b = m^2/m_0^2$ for the quanta/gap ratio. Changing integration variables $t \rightarrow u$ such that $4ut = z^2$, one gets

$$\bar{P}(x) = \frac{3}{16\pi^2} \int_0^{\infty} du \left(\frac{\partial^2}{\partial x^2} \left[\frac{4}{x_E^2} \exp\left(-\frac{x_E^2 m_0^2}{4u}\right) \right] \right) \cdot \frac{\exp(-u)}{(1 - \exp(-bu))^2} (1 + \exp(-bu)(b-1)) \quad (71)$$

Performing differentiation, we finally obtain

$$\bar{P}(x) = -\frac{3m_0^4}{16\pi^2} \bar{p}_b(z) \quad (72)$$

where the universal function $\bar{p}_b(z)$ has the following form

$$\bar{p}_b(z) = \int_0^{\infty} \frac{du}{u^2} \exp\left(-\frac{z^2}{4u} - u\right) \frac{1 + \exp(-bu)(b-1)}{(1 - \exp(-bu))^2} \quad (73)$$

This result has been used in the main text.

For scalar and pseudoscalar channels one also needs the function $\hat{P}(x)$ defined as

$$\hat{P}(x) = -i \int \frac{d^4 q}{(2\pi)^4} \sum_{n=0}^{\infty} \frac{1}{-q^2 + m_n^2} \exp(-iqx) \quad (74)$$

where again $m_n^2 = m_0^2 + m^2 n$. Performing completely analogous calculations one gets

$$\hat{p}_b(z) = 4\pi^2 x_E^2 \hat{P}(x) = \int_0^{\infty} du \exp\left(-\frac{z^2}{4u} - u\right) \frac{1 + \exp(-bu)(b-1)}{(1 - \exp(-bu))^2} \quad (75)$$

The short-distance asymptotics of $\bar{p}_b(z)$ can be easily found from the definition (73), it is given by:

$$\bar{p}_b(z) = \frac{128}{b} \cdot \frac{1}{z^6} + \left(2 - \frac{2}{b} - \frac{b}{3}\right) \cdot \frac{1}{z^2} + \frac{3b - 2 - b^2}{6b} \log z^2 + \dots \quad (76)$$

where the dots denote constant (z^2 -independent) term and positive powers of z^2 .

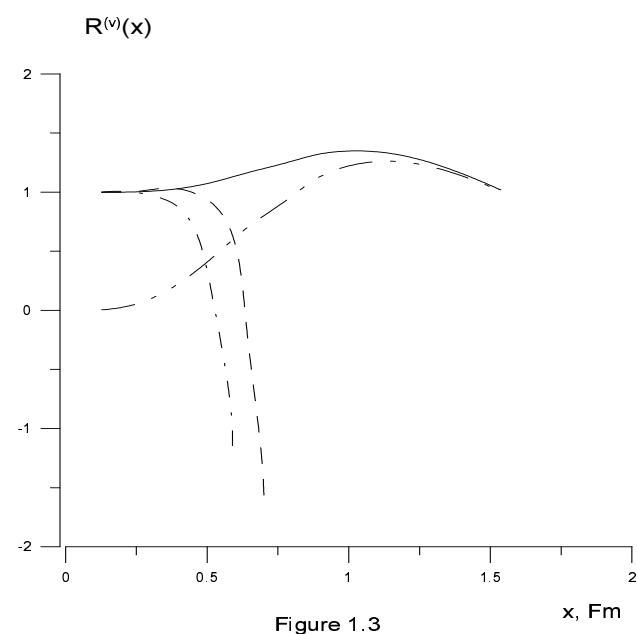
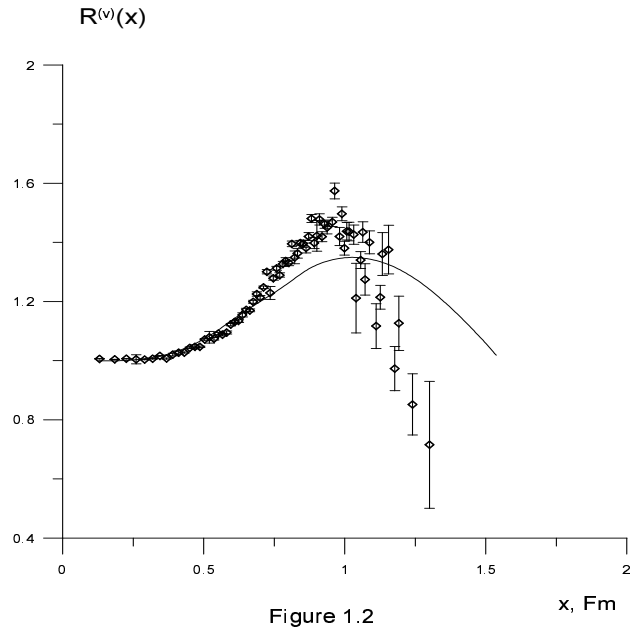
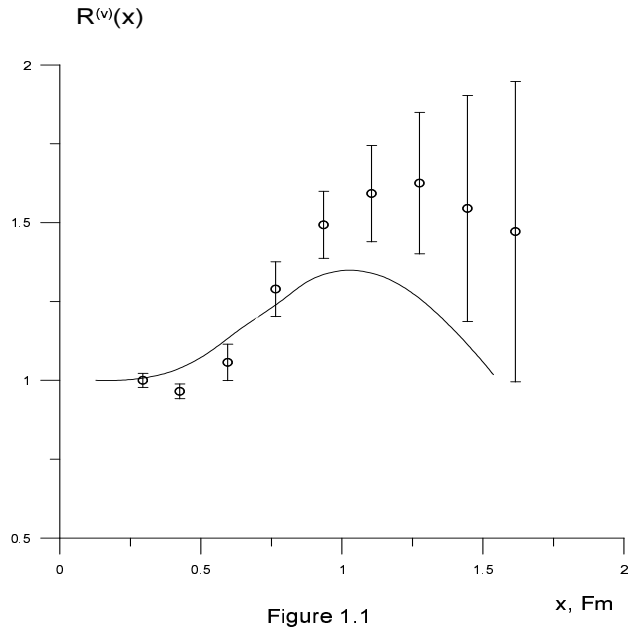
References

- [1] F.J.Yndurain, *Quantum Chromodynamics: The Theory of Quark and Gluon Interactions*, Springer, 1999.
- [2] M. A. Shifman, A. I. Vainshtein and V. I. Zakharov, Nucl. Phys. B **147** (1979) 385; 448.
- [3] M. C. Chu, J. M. Grandy, S. Huang and J. W. Negele, Nucl. Phys. Proc. Suppl. **30** (1993) 495 [arXiv:hep-lat/9211012].
- [4] T. DeGrand, Phys. Rev. D **64** (2001) 094508 [arXiv:hep-lat/0106001].
- [5] E. V. Shuryak, Nucl. Phys. B **319** (1989) 521, 541; E. V. Shuryak, Nucl. Phys. B **328** (1989) 85, 102
- [6] K.G. Chetyrkin , S. Narison, V. I. Zakharov, *Nucl.Phys.B* **550** (1999) 353
- [7] V. Shevchenko and Yu. Simonov, Phys. Rev. D **65** (2002) 074029 [arXiv:hep-ph/0109051].
- [8] R. Hofmann, Prog. Part. Nucl. Phys. **52** (2004) 299 [arXiv:hep-ph/0312130].
- [9] G. 't Hooft, Nucl. Phys. B **72** (1974) 461; E. Witten, Nucl. Phys. B **149** (1979) 285.
- [10] E. De Rafael, AIP Conf. Proc. **602** (2001) 14 [arXiv:hep-ph/0110195].
- [11] B. Lucini, M. Teper and U. Wenger, arXiv:hep-lat/0401028.
- [12] Yu. A. Simonov, Phys. Atom. Nucl. **66** (2003) 2038 [Yad. Fiz. **66** (2003) 2088] [arXiv:hep-ph/0210309]; A. M. Badalian, B. L. G. Bakker and Y. A. Simonov, Phys. Rev. D **66** (2002) 034026 [arXiv:hep-ph/0204088].
- [13] P. Cea, P. Colangelo, L. Cosmai and G. Nardulli, Phys. Lett. B **206** (1988) 691.
- [14] Yu. A. Simonov, arXiv:hep-ph/0305281
- [15] Y. A. Simonov, in *Lectures Notes in Physics*, v.479, p.139, Springer, 1996; A. M. Badalian and Yu. A. Simonov, Phys. Atom. Nucl. **60** (1997) 630 [Yad. Fiz. **60** (1997) 714].
- [16] M. A. Shifman, arXiv:hep-ph/0009131; I. I. Y. Bigi and N. Uraltsev, Int. J. Mod. Phys. A **16** (2001) 5201 [arXiv:hep-ph/0106346]; S. Jeschonnek and J. W. Van Orden, arXiv:hep-ph/0209157.
- [17] A. Y. Dubin, A. B. Kaidalov and Yu. A. Simonov, Phys. Lett. B **323** (1994) 41.

- [18] M. Golterman and S. Peris, Phys. Rev. D **67** (2003) 096001 [arXiv:hep-ph/0207060]; M. Golterman, S. Peris, B. Phily and E. De Rafael, JHEP **0201** (2002) 024 [arXiv:hep-ph/0112042]; M. Golterman and S. Peris, JHEP **0101** (2001) 028 [arXiv:hep-ph/0101098].
- [19] S. R. Beane, Phys. Rev. D **64** (2001) 116010 [arXiv:hep-ph/0106022]
- [20] S. S. Afonin, A. A. Andrianov, V. A. Andrianov and D. Espriu, JHEP **0404** (2004) 039 [arXiv:hep-ph/0403268]; S. S. Afonin, Phys. Lett. B **576** (2003) 122 [arXiv:hep-ph/0309337].
- [21] V. A. Novikov, M. A. Shifman, A. I. Vainshtein and V. I. Zakharov, Nucl. Phys. B **249** (1985) 445 [Yad. Fiz. **41** (1985) 1063].
- [22] K. G. Chetyrkin, A. A. Pivovarov, Nuovo Cimento, A **100** (1988) 899.
- [23] A. Bramon, E. Etim and M. Greco, Phys. Lett. B **41** (1972) 609.
- [24] J. J. Sakurai, Phys. Lett. B **46** (1973) 207.
- [25] G. Veneziano, Nuovo Cim. A **57** (1968) 190.
- [26] Yu. A. Simonov, Phys. Atom. Nucl. **58** (1995) 107 [arXiv:hep-ph/9311247].
- [27] Yu. A. Simonov, *Phys. Atom. Nucl.* **65** (2002) 135 [arXiv:hep-ph/0109081].
- [28] S. R. Beane, Phys. Lett. B **521** (2001) 47 [arXiv:hep-ph/0108025].
- [29] T. J. Allen, C. Goebel, M. G. Olsson and S. Veseli, Phys. Rev. D **64** (2001) 094011 [arXiv:hep-ph/0106026].
- [30] Yu. A. Simonov, *in preparation*
- [31] Y. A. Simonov, arXiv:hep-ph/9911237.
- [32] S. Narison and V. I. Zakharov, Phys. Lett. B **522** (2001) 266 [arXiv:hep-ph/0110141].
- [33] Y. A. Simonov, Phys. Atom. Nucl. **67** (2004) 846 [Yad. Fiz. **67** (2004) 868] [arXiv:hep-ph/0302090].
- [34] B.V. Geshkenbein, B.L. Ioffe, K.N. Zyablyuk, *Phys.Rev. D* **64** (2001) 093009
- [35] Th. Schaefer, E. Shuryak, *Phys.Rev.Lett.* **86** (2001) 3973
- [36] E. de Rafael, Nucl. Phys. Proc. Suppl. **96** (2001) 316 [arXiv:hep-ph/0010209]; S. Peris, B. Phily and E. de Rafael, Phys. Rev. Lett. **86** (2001) 14 [arXiv:hep-ph/0007338].

Figure captions

- Fig. 1.1 Lattice data from [3] for the vector channel correlator vs expression (14).
- Fig. 1.2 Lattice data from [4] for the vector channel correlator vs expression (14).
- Fig. 1.3 Expression (14) (solid curve) together with its own short distance expansion (17) (dashed-dotted curve) and short distance OPE expansion (20) (dashed curve). The lightest resonance contribution is also shown (double dotted curve).
- Fig. 2.1 Lattice data from [3] for the axial channel correlator vs expression (30).
- Fig. 2.2 Lattice data from [4] for the axial channel correlator vs expression (30).
- Fig. 2.3 Expression (30) (solid curve) together with its own short distance expansion (31) (dashed-dotted curve) and short distance OPE expansion (32) (dashed curve).
- Fig. 3.1 Lattice data from [3] for the pseudoscalar channel correlator vs expression (39).
- Fig. 3.2 Lattice data from [4] for the pseudoscalar channel correlator vs expression (39).
- Fig. 3.3 Expression (39) (solid curve) together with its own short distance expansion (41) (dashed-dotted curve) and short distance OPE expansion (42) (dashed curve).
- Fig. 3.4 Expression (39) for different values of the parameter a : $a = 2$ (upper curve), $a = 0$ (solid curve) and $a = -1$ (lower curve).
- Fig. 4.1 Lattice data from [3] for the scalar channel correlator vs expression (48) for different values of a : $a = 2$ (upper curve), $a = 1$ (middle curve) and $a = 0$ (lower curve).
- Fig. 4.2 Lattice data from [4] for the scalar channel correlator vs expression (48).
- Fig. 4.3 Expression (48) (solid curve) together with its own short distance expansion (50) (dashed-dotted curve) and short distance OPE expansion (49) (dashed curve).



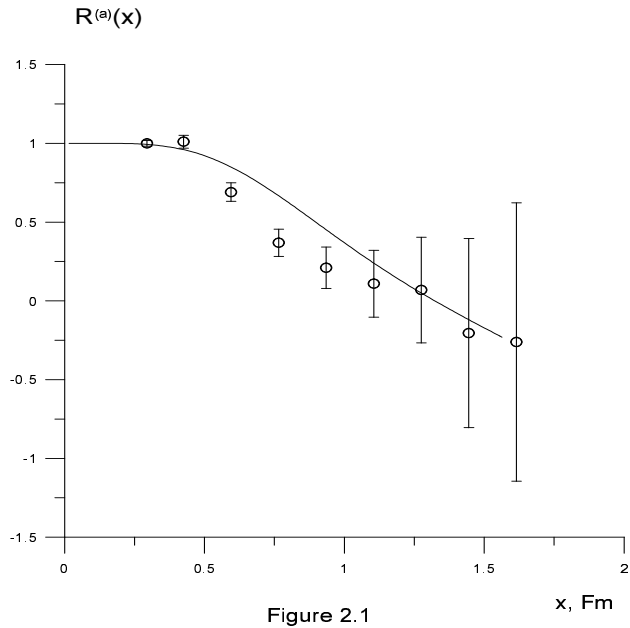


Figure 2.1

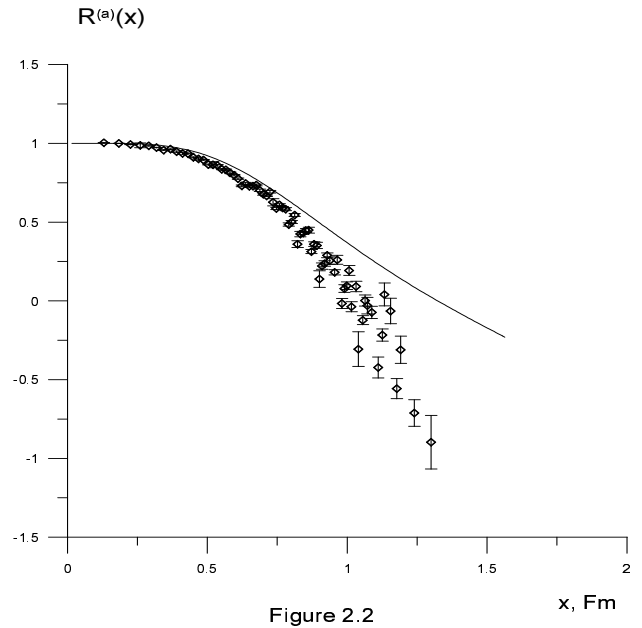


Figure 2.2

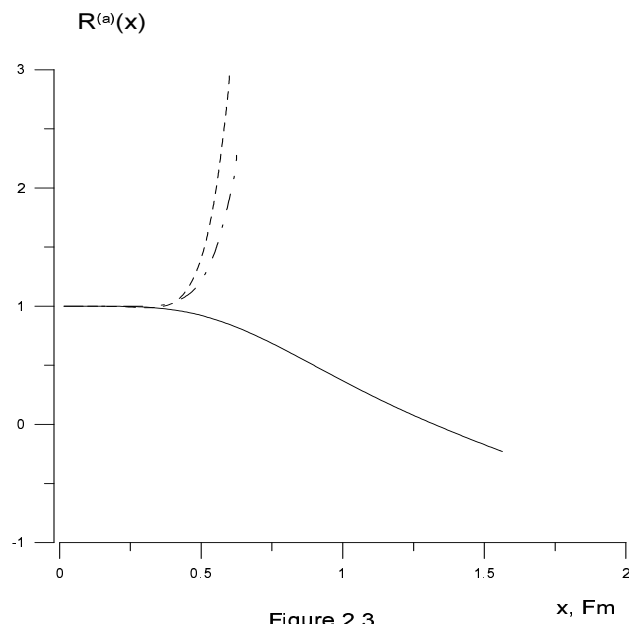
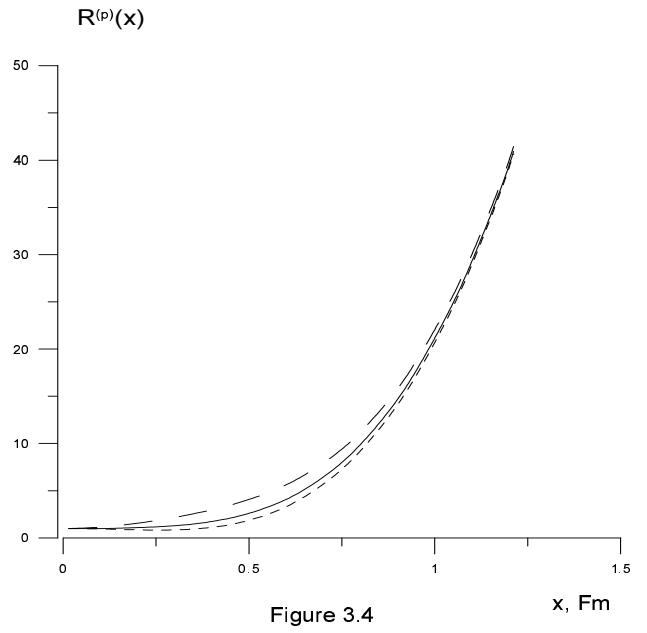
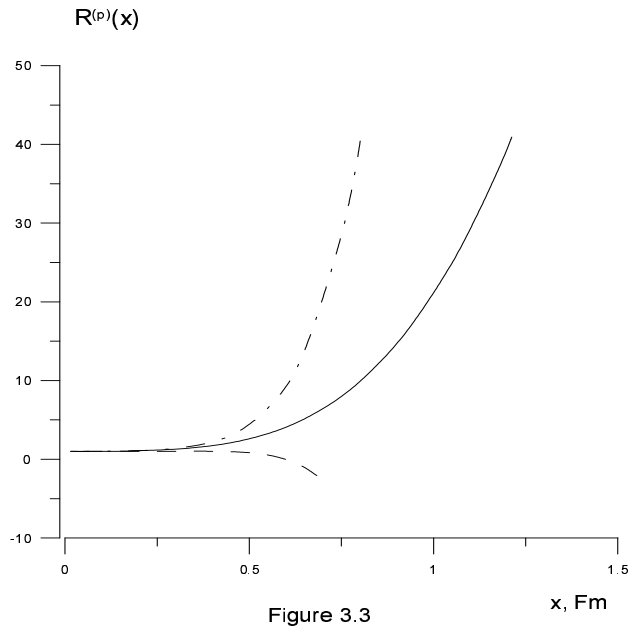
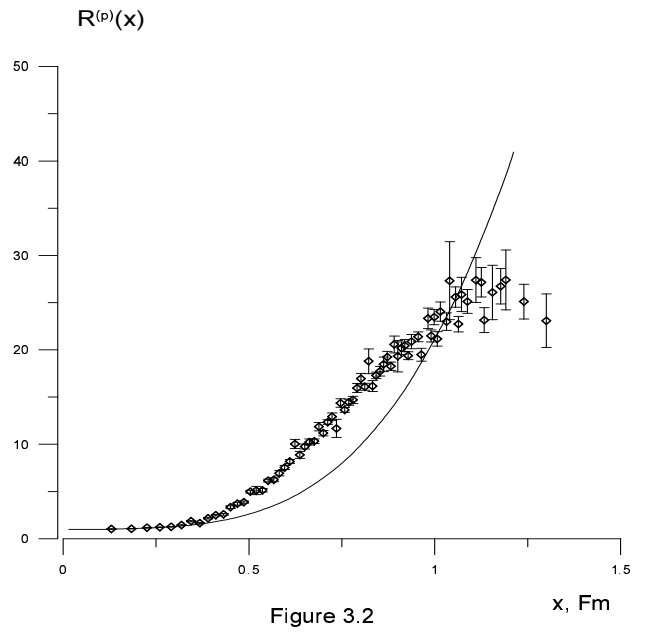
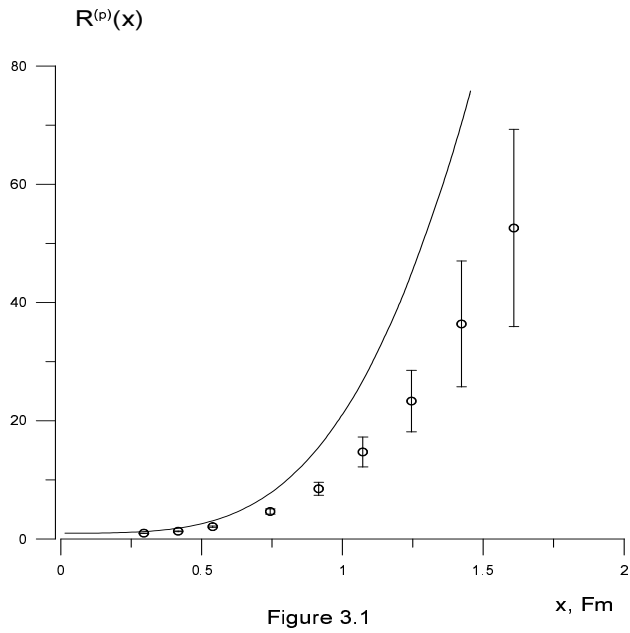


Figure 2.3



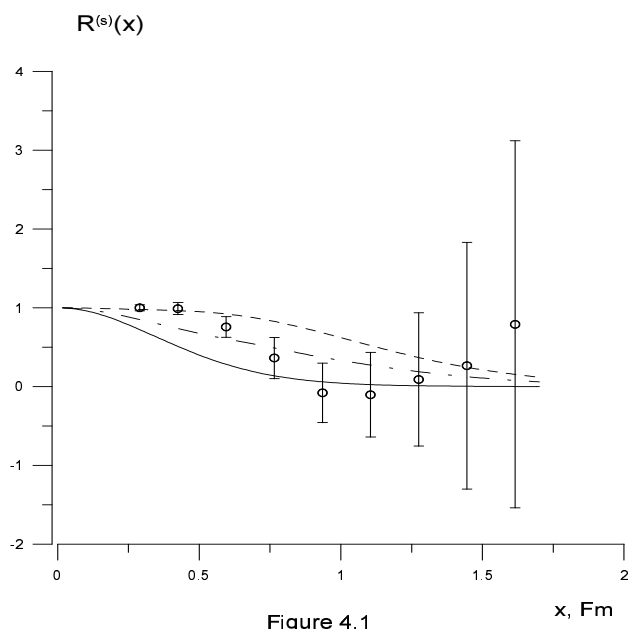


Figure 4.1

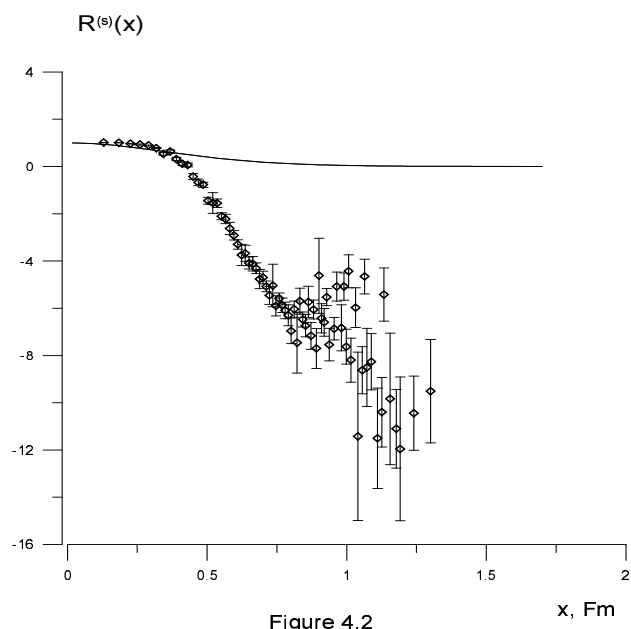


Figure 4.2

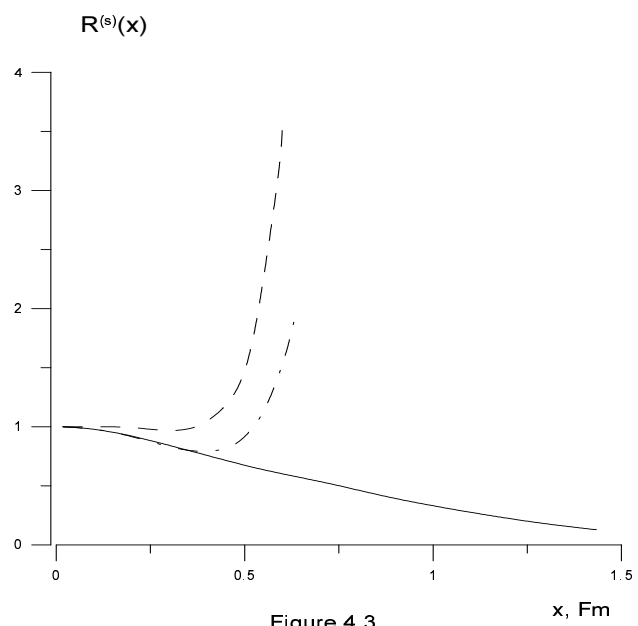


Figure 4.3